Enhanced photocatalytic behaviour of KOH treated TiO_2 nanotubes via electrochemical anodization process

SYAZWAN HANANI BINTI MERIAM SUHAIMY[a,b,c], SHARIFAH BEE ABD HAMID[*,a], CHIN WEI LAI[a], MD. RAKIBUL HASAN[a], MOHD RAFIE JOHAN[b]

[a]*Nanotechnology and Catalysis Research Centre (NANOCAT), Institute of Postgraduate Studies (IPS), University of Malaya, 50603 Kuala Lumpur, Malaysia*

[b]*Nanomaterials Engineering Research Groups, Advanced Materials Research Laboratory, Department of Mechanical Engineering, University Malaya, 50603 Kuala Lumpur, Malaysia*

[c]*Faculty of Science, Technology and Human Development, Universiti Tun Hussein Onn Malaysia, UTHM, Parit Raja, Batu Pahat 86400, Johor, Malaysia*

TiO_2 nanotube arrays have attracted great interest as the promising candidate for photcatalytic degradation of organic pollutants. In the present study, the incorporation of 1.6wt% of 1M potassium hydroxide in a fluorinated-ethylene glycol electrolyte could fabricate a high aspect ratio (≈ 21) TiO_2 nanotube arrays film via electrochemical anodization technique at 30V for 1 hour. Theoretically, the growth of TiO_2 nanotube arrays and their photocatalytic activity could further improved by simple addition of an optimum content of potassium hydroxide into the fluorinated-ethylene glycol electrolyte. It was believed that the presence of optimum content of potassium species into the lattice of TiO_2 acted as electron acceptor to enhance the transportation of charge carriers, where the photo-induced electron-hole pairs transfer by excitation separated electrons and holes effectively under illumination. Based on the results obtained, the modified potassium-loaded TiO_2 nanotube film exhibited high photocurrent density of 0.57 mA/cm^2 and showed high photocatalytic degradation of 5ppm methyl orange dye (100%) after 10 minutes irradiation time.

(Received September 29, 2015; accepted October 28, 2015)

Keywords: TiO_2 nanotube arrays, Anodization, Photocatalytic activity, Photodegradation, Potassium hydroxide

1. Introduction

Reliable and sustainable water supply is essential for all living beings in the world. It is an important source for agriculture, electric power production, manufacturing, and even for domestic usage. Domestic use of water includes bathing, laundry, washing clothes, other household activities and even for drinking. As such, it is understood that a source of safe and clean drinking water is an important issue to meet basic human needs, so that, a healthy body could function well. However, the misuse and subsequent direct and indirect have inadvertently released to the environment. In Malaysia, the pollution of drinking water has yet to be examined. Therefore, synthesizing photocatalyst in order to remove selected contaminants in drinking water is needed. Photocatalytic degradation is considered to be one of effective ways in breaking down organic compounds to carbon dioxide and water. The most commonly used photocatalyst is the fascinating Titanium Dioxide (TiO_2) due to its availability in low-cost, resistant to corrosion, long term stability, practically non-toxic and high photo reactivity [1-4]. However, a wide band gap of TiO_2 restricts its utilization of the ultra-violet light and high recombination rate of charge carriers results in lower reaction rates for photocatalytic degradation process [5-8]. Therefore, intense efforts have been made to alter the electronic and optical properties of TiO_2 nanotubes by narrowing the band gap [9-13]. In 2001, Grimes and co-workers [14] first reported the porous of titania nanotube arrays formed in an hydrofluoric (HF) electrolyte via anodic oxidation process. The use of different organic solvents offers the control of the nanotubes structure. In 2005, it appears that, smooth tubes can be grown to much higher aspect ratios and show a strongly improved ordering in non-aqueous electrolytes [15]. In the next year later, formation of smaller diameter with very high aspect ratio, reported by Macak and Schmuki [16] using fluoride containing organic electrolytes ,ethylene glycol was reported. This study is focused on controlling the growth performance of TiO_2 nanotubes by using potassium hydroxide (KOH). In this present study, potassium hydroxide is added to the mixture of NH_4F and EG solutions to prepare TiO_2 nanotubes through anodic oxidation method and the morphology together with it's photodegradation performance has been explored.

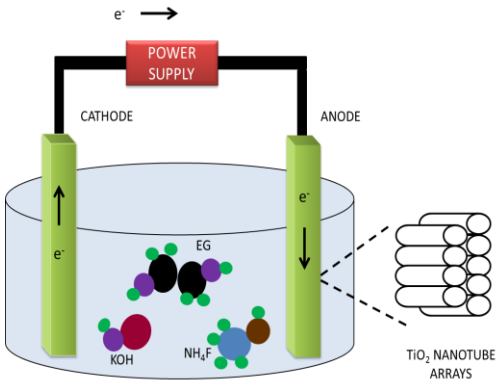

Fig. 1. Illustrative drawing of the experimetal setup for anodization process

2. Experimental procedure

In the present study the K-incorporated TiO_2 NTs was prepared via anodization process. Titanium foils with the thickness of 0.127mm, 99.7% from Sigma – Aldrich were used. The Ti foil was cut into (1cm x 5cm) dimension for each anodization process. Firstly, ammonium fluoride (NH_4F) in the form of solid was dissolved in Ethylene Glycol (EG). Different amount of potassium hydroxide (KOH) was added to the mixture of NH_4F and EG and stirred for one hour. Anodizing was conducted in a bath containing NH_4F + EG with additions of 0.4, 0.8, 1.2, 1.6 and 2.0 wt% KOH. In an anodizing cell, the titanium foil is made as the anode by connecting to the positive terminal of direct current power supply. The cathode is a platinum electrode and connected to the negative terminal of the supply. When the circuit is closed, electrons are withdrawn from the metal at the positive terminal allowing ions at the metal to react with electrolytes to form an oxide layer on the titanium foil as shown in Fig. 1. All samples were anodized at 30V for 1 hour. After anodization, ethanol and deionized water were used as the cleaning agent in the cleaning process to remove the remaining electrolytes on the nanotubes and try to eliminate the precipitation on top of the nanotubes. To induce crystallinity, the samples were heated at 450℃ for 1 hour. Annealed samples were then dispersed in a quartz tube containing 60 mL of 5ppm Methyl Orange (MO) aqueous solution. Adsorption-desorption equilibrium is promoted by keeping the mixture in the dark for 30 min before get expose to UV irradiation. The visible light source was a 96W UV lamp. Next step was to characterize the samples by various analytical techniques. Scanning Electron Microscope, using FEI Quanta 200F, was used to examine the structural morphology and particle size of the sample. The crystal structure and the degree of crystallinity of the samples were characterized by using X-Ray Diffraction (XRD). The XRD was performed with Cu Kα radiation (α = 1.5406 Å) on a Bruker axs D8 Advance diffractometer from 20° to 70°. Raman spectroscopy has been used for material phase examination. Autolab potentiostat (Ecochemie, Netherlands) was used to measure the photocurrent response of the samples. A 150W solar simulator was used as a light source. A schematic diagram presents the preparation of TiO_2 nanotube arrays is shown in Fig. 2.

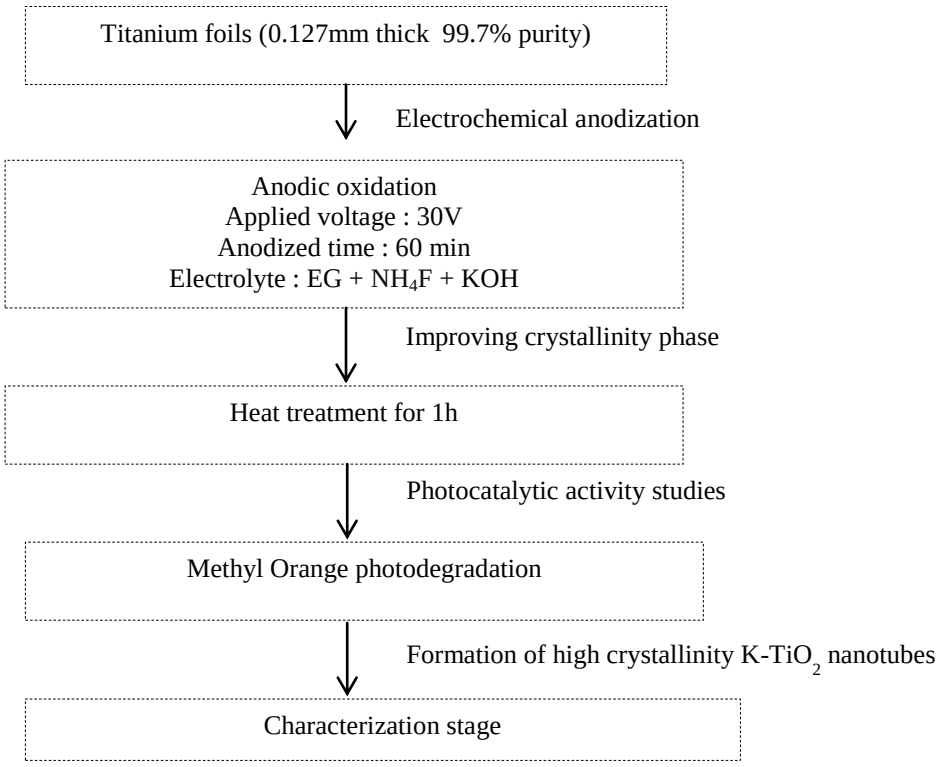

Fig. 2. Schematic diagram of the preparation of TiO_2 nanotube arrays

3. Results and discussion

Morphological studies. Fig. 3 shows the top view of nanotube arrays and insets are the cross-section morphology of Ti anodized. It is observed that the nanotube arrays were successfully synthesized during anodization and each sample has similar morphology, grown vertically from Ti substrate, showing open ended tubes and closely packed in structure as compared to TiO_2 nanotube arrays formed in electrolyte without KOH as observed by Syazwan Hanani *et al* in 2015 [17]. The finding showed that with the addition of KOH, the pore diameter of TiO_2 nanotube arrays is increased. As can be seen in Figure 3, the pore diameters were gradually increased uniformly with the increase of KOH concentration until 1.6%. But at 2.0% KOH, again the irregular porous layer was formed. Significant changes were also observed in the ordered oxide layer of the samples. As tabulated in Table 1, the nanotubular structure synthesized with 2.0wt% of KOH exhibited nanotubes of ~1.96µm lengths. Meanwhile, the longest tube length was observed in the samples synthesized with 1.6wt% of KOH. Although low aspect ratio was calculated due to variation in pore diameters, remarkable photocatalytic performance was observed and described in the later part.

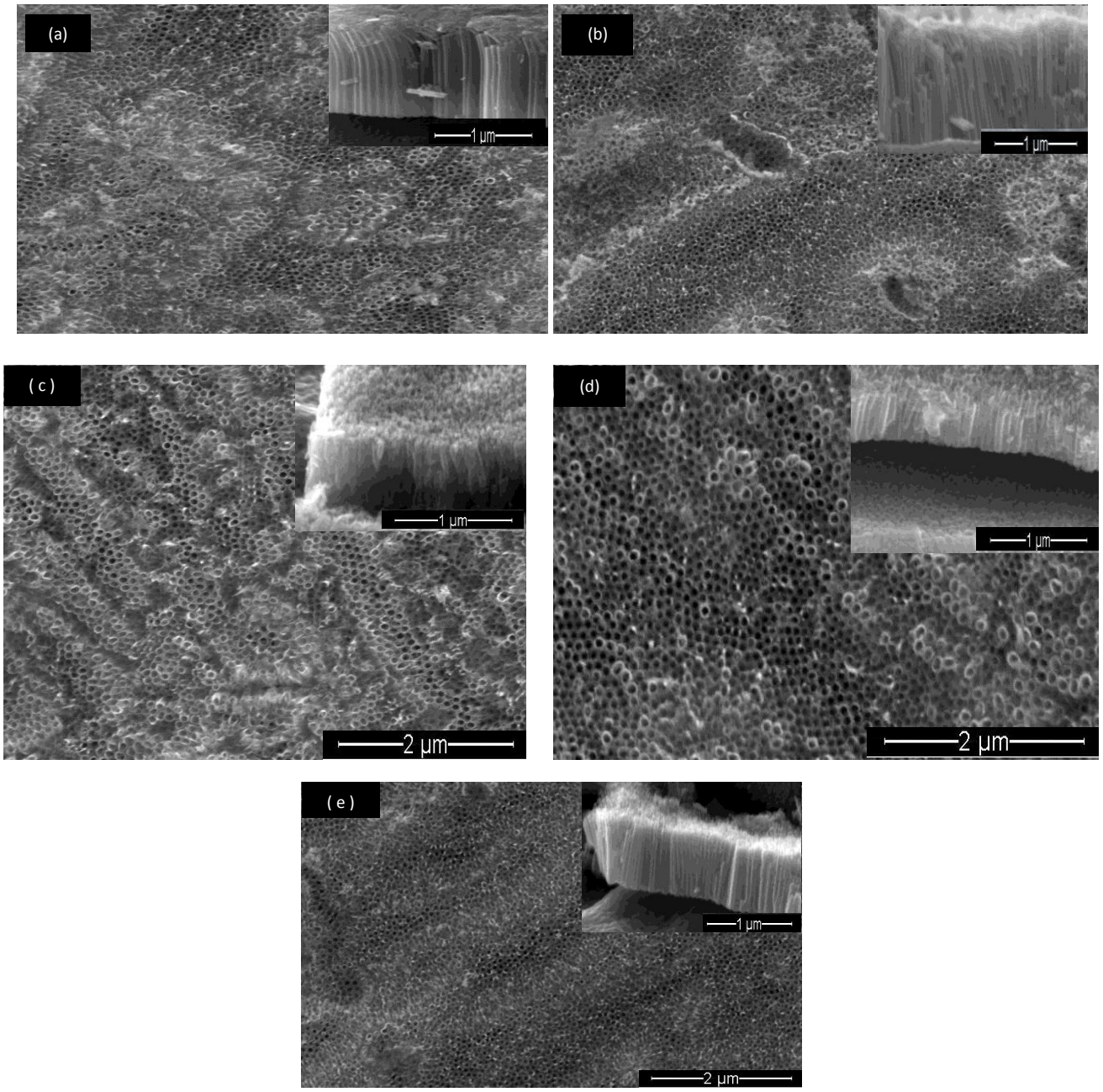

Fig. 3. SEM images of TiO_2 nanotubes arrays at different amount of KOH (a) 0.4wt% (b) 0.8wt% (c) 1.2wt% (d) 1.6wt% (e) 2.0wt%

Table 1. Structural characteristic of TiO_2 nanotube arrays in different amount of KOH

Amount of KOH(g)	Tube length (µm)	Pore diameter (nm)	Aspect Ratio
0.4wt%	0.51±0.03	84.07 ± 6.06	6
0.8wt%	0.80 ±0.01	102.24 ± 2.51	8
1.2wt%	0.88 ±0.01	69.61 ± 9.27	13
1.6wt%	2.00 ±0.1	95.27 ±18.45	21
2.0wt%	1.96 ±0.27	89.05 ±7.45	22

Fig. 4 shows the diffraction patterns of TiO_2 NTs at different amount of KOH after heat treatment at 450℃ for 1 hour. We can observe the Ti and anatase peaks with no other secondary phases. Peaks from Ti were at 2θ of 38.5°, 43.77°, 55.5°, 64° while peaks from anatase TiO_2 were at 2θ of 25.5°, 33.77°, 48°.

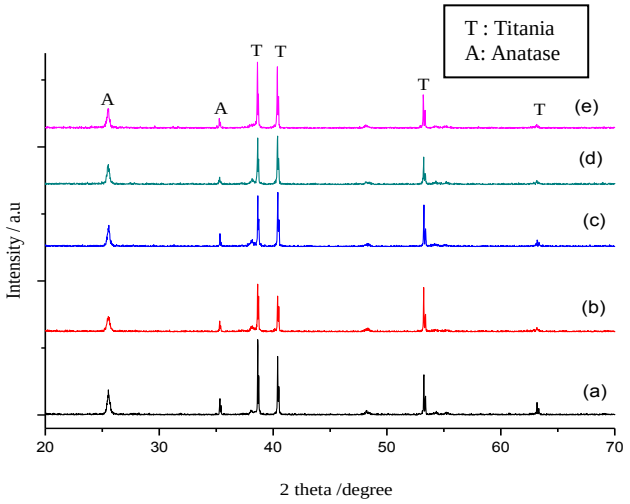

Fig. 4. XRD patterns of TiO_2 nanotubes at different amount of KOH. (a) 0.4wt%, (b) 0.8wt%, (c) 1.2wt%, (d) 1.6wt%, (e) 2.0wt%

From the results, sharp and strong peaks were observed in higher concentration of KOH whereas 0.4wt% KOH shows comparatively weak peaks. 1.6% KOH treated samples exhibited better crystallization. KOH is considered can enhance TiO_2 nanotubes growth by reducing the acidity of the electrolytes. Such OH groups can considerably affect the formation of anatase-crystallites by the interaction between the dissociated H_2O molecules and OH group of octahedral in TiO_2 [18]. However, the addition of OH^- in larger amounts restrains the growth of TiO_2 nanotubes upon chemical dissolution:

$$TiO_2 + 6F^- + 4H^+ \rightarrow [TiF_6]^{2-} + 2H_2O$$

through lowered down the H^+ concentration [19]. This effect is obvious when 2.0wt% KOH was used and the tube length became shorter. To further confirm the anatase phase and crystalline nature of the sample, Raman spectra analysis was also recorded.

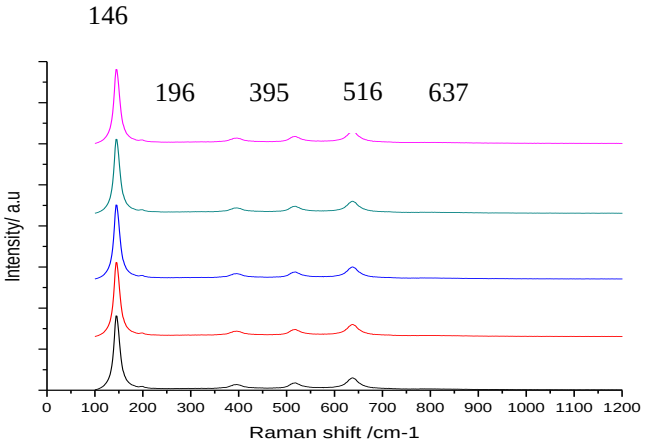

Fig. 5 Raman spectra of TiO_2 nanotube arrays at different amount of KOH. (a) 0.4wt%, (b) 0.8wt%, (c) 1.2wt%, (d) 1.6wt%, (e) 2.0wt%

Six irreducible representation of the optical active modes for anatase which are ($3E_g + 2B_{1g} + A_{1g}$) [20], indicating the formation of well crystallized anatase as shown in Figure 5. This is in good agreement with XRD results shown in Figure 4. In the present study, three Eg modes give typical scattering at 146 (main band), 196, and 637 cm^{-1}. The spectrum also exhibit two B_{1g} modes at 395 and 516 cm^{-1} overlapping with one mode of A_{1g} at 516cm^{-1}. Studies show that the Eg mode is sensitive to oxygen deficiencies. The strongest Eg mode at 146cm^{-1} is due to the symmetric bending vibration of O–Ti–O bonds. The symmetric and anti-symmetric bending vibration of O–Ti–O bond explains the B_1g and A_1g modes. The sharp peak at 146 cm^{-1} explains the crystallinity of nanotubes.

Table 2. Elemental analysis of anodic TiO_2 nanotubes at different amounts of KOH.

Sample	Element	Weight %	Atomic%
0.4wt%	O	11.07	64.57
	Ti	17.60	35.42
0.8wt%	O	11.93	66.24
	Ti	18.2	33.76
1.2wt%	O	11.79	64.45
	Ti	19.46	35.55
1.6wt%	O	11.64	67.1
	Ti	17.09	32.9
2.0wt%	O	9.62	61.07
	Ti	18.35	38.93

The elemental analysis of each samples are provided in Table 2. Ti and O are the major elements in each sample showing that the nanotube arrays are composed of titanium oxide. Furthermore, the highest content of O for 1.6wt% KOH sample translates the thicker amount of oxide layer among the other samples.

A typical photocurrent response was examined by current-voltage diagram as shown in Fig. 6. The photo response was varied significantly with different amount of KOH under irradiated condition.

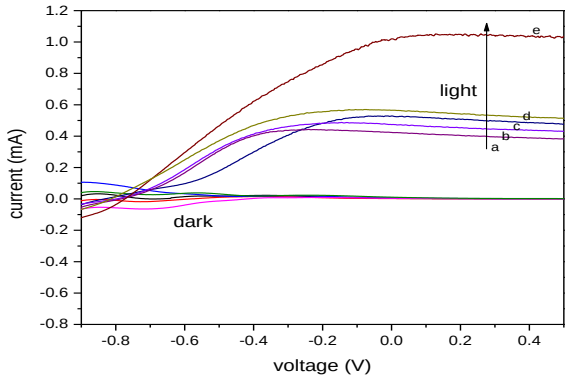

Fig. 6. Current-voltage diagram of KOH treated TiO_2 at different amount of KOH. (a) 0.4wt%, (b) 0.8wt%, (c) 1.2wt%, (d) 1.6wt%, (e) 2.0wt%

Sample with 0.4wt% KOH (a) shows lower photocurrent response of ~0.44mA/cm^2. Maximum photocurrent density was recorded ~1.04mA/cm^2 for 2.0wt% KOH (e) treated sample. The reason may be attributed to the higher crystallinity of the samples at higher concentrations of KOH. Since crystalline of TiO_2 structure can reduce charge transfer resistance significantly which eventually enhances the electron mobility throughout the surface [21]. Interestingly, 1.6wt% KOH treated sample showed better photocatalytic performance although lower photocurrent density (0.57mA/cm^2) was observed. This phenomenon could be attributed to optimum aspect ratio of the sample. Previous studies showed that recombination of the charge carriers at very high aspect ratio restricts the photocatalytic efficiency [22].

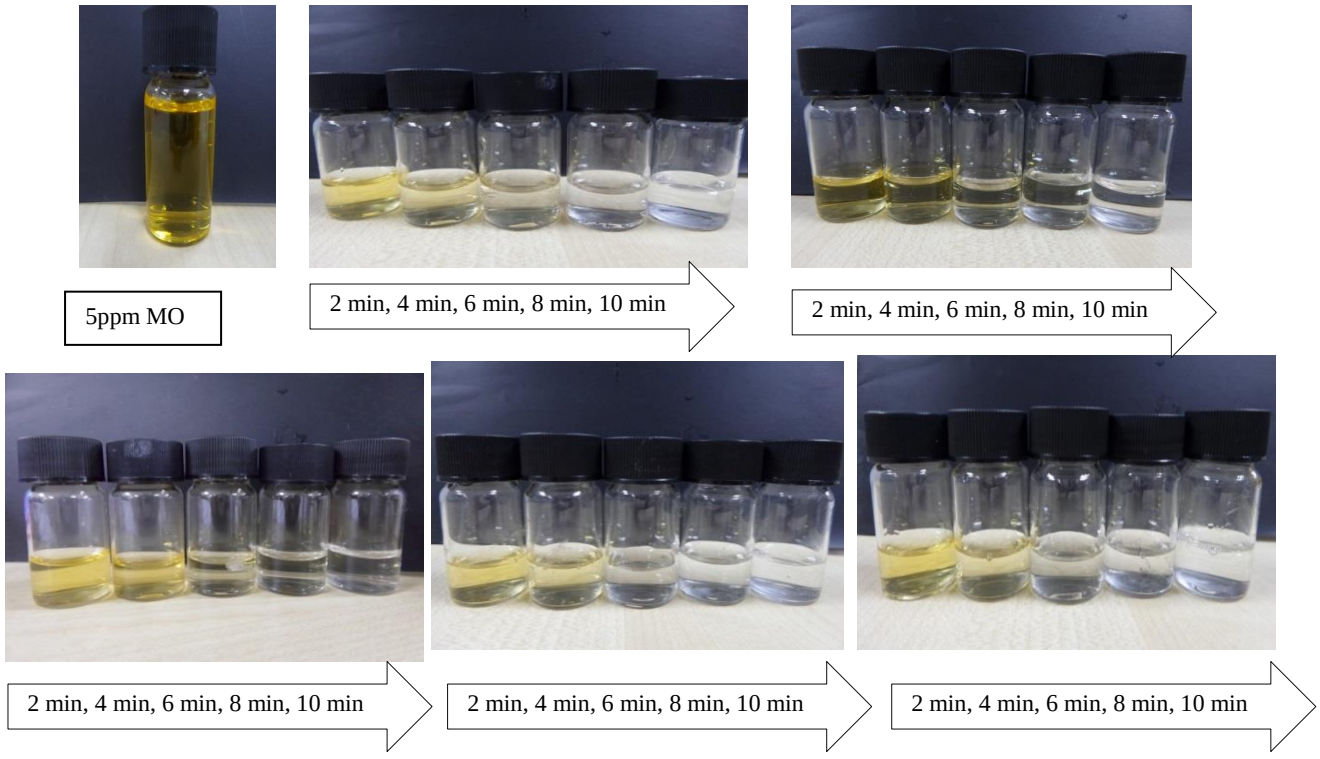

Fig. 7. The colour changing of MO in 2 min interval time for different amount of KOH a) 0.4 wt% b) 0.8wt% c) 1.2 wt% d) 1.6wt% e) 2.0wt%

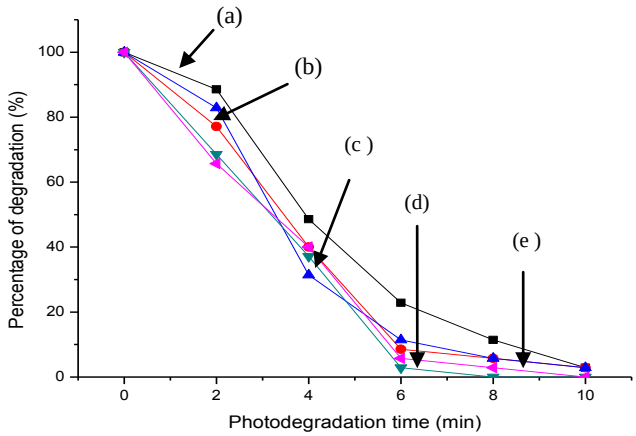

Fig. 8. Optical absorbance versus time for samples with a) 0.4 wt% b) 0.8wt% c) 1.2 wt% d) 1.6wt% e) 2.0wt% KOH

Fig. 7 shows the photodegradation performance which was investigated by the degradation of Methyl Orange. The purpose of this experiment is to study which sample gives the best degradation in 10 minutes under photo irradiation. The colour was varied of each sample when MO was irradiated by UV light for 10 min in the absence of photocatalyst. Specific degradation of all samples was observed as shown by the decrease in the absorbance in Fig. 8. Based on the results obtain, we could see that 1.6wt% KOH contained electrolyte possessed good photo-degradation with no color of Methyl Orange at 6 min. From these results, the absorbance for all samples decrease with time and the most suitable concentration of KOH to be added in electrolyte is 1.6wt% as the absorbance is almost 0 at after 8 minutes. It shows that the sample has the greatest reaction rate and exhibit positive effect on MO absorbance. The degradation efficiency of MO is possessed by the decomposing power of the positive holes. Water is oxidized at the positive holes of valence bands to release hydroxyl radicals (•OH) which then reacts with MO solutions and finally decompose to carbon dioxide and water. This indicated that the formed TiO_2 nanotube arrays have the availability to create electron-hole pairs [23].

4. Conclusions

In summary, TiO_2 nanotube arrays which was fabricated via anodization at 30V for 1 h in potassium hydroxide added fluorinated-ethylene glycol electrolyte work as an efficient photocatalyst. High aspect ratio (≈21) TiO_2 nanotube arrays has the ability to degrade 5ppm methyl orange dye after 10 minutes ultra violet irradiation time. It was also found that TiO_2 nanotube arrays modified with the addition of KOH in electrolyte exhibited high photocurrent density of ~0.57 mA/cm^2 and showed high photocatalytic degradation of 5ppm methyl orange dye (100%) after 10 minutes irradiation time. This simple technique of preparation of reusable and high active photocatalyst thin films will be promising in future generation water treatment process.

Conflicts of interest

The authors declare that they have no conflict of interests regarding the publication of this paper.

Acknowledgements

The authors would like to thank University of Malaya for funding this research work under Postgraduate Research Fund (PPP: PG034-2013B), University of Malaya Research Grant (UMRG: RP022- 2012A and RP022-2012D), Universiti Tun Hussein Onn and Ministry of Higher Education, Malaysia.

References

[1] A. Fujishima, T. N. Rao, D. A. Tryk, Journal of Photochemistry and Photobiology C: Photochemistry Reviews,. **1**(1), 1 (2000).
[2] N. Serpone, E. Pelizzetti, 1989: Wiley New York.
[3] M. Schiavello, Photoelectrochemistry, photocatalysis and photoreactors, fundamentals and developments. 1985.
[4] A. L. Linsebigler, G. Lu, J. T. Yates Jr, Chemical reviews, **95**(3), 735 (1995).
[5] X. Quan, et al., Environmental science & technology, **39**(10), 3770 (2005).
[6] W. Ho, C. Y. Jimmy, S. Lee, Journal of solid state chemistry, **179**(4), 1171 (2006).
[7] W. H. Ryu, C. J. Park, H. S. Kwon, Journal of nanoscience and nanotechnology, **10**(5), 3671 (2010).
[8] V. Kislyuk, O. Dimitriev, Journal of nanoscience and nanotechnology, **8**(1), 131 (2008).
[9] B. H. Meekins, P. V. Kamat, ACS nano, **3**(11), 3437 (2009).
[10] B. Zhu, et al., Journal of molecular catalysis A: chemical, **249**(1), 211 (2006).
[11] A. Fujishima, X. Zhang, D. A. Tryk, Surface Science Reports, **63**(12), p. 515 (2008).
[12] M. Ni, M. K. Leung, D. Y. Leung, International Journal of Hydrogen Energy, **32**(13), 2305 (2007).
[13] D. Ke, et al., Materials Letters, **62**(3) 447 (2008).
[14] D. Gong, et al., Z. Chen, E. C. Dickey, J. Mater. Res., **2001**, 16 (2001).
[15] J. M. Macak, et al., Angewandte Chemie International Edition, **44**(45), 7463 (2005).
[16] J. M. Macak, P. Schmuki, Electrochimica Acta, **52**(3), 1258 (2006).
[17] M. Suhaimy, et al. Advanced Materials Research. 2015. Trans Tech Publ.
[18] L.-M. Liu, P. Crawford, P. Hu, Progress in Surface Science, **84**(5), 155 (2009).

[19] Y. Wang, et al., Journal of Alloys and Compounds, **509**(14), L157 (2011).
[20] T. Ohsaka, F. Izumi, Y. Fujiki, Journal of Raman Spectroscopy, **7**(6), 321 (1978).
[21] M. R. Hasan, S. B. A. Hamid, W. J. Basirun, Applied Surface Science, **339**, 22 (2015).
[22] W. Krengvirat, , et al., Electrochimica Acta, **89**, 585 (2013).
[23] C. W. Lai, S. Sreekantan, Materials Science in Semiconductor Processing, **16**(2), 303 (2013).

*Corresponding author: sharifahbee@um.edu.my